Analytic Equation of State and Thermodynamic Properties of Solid FCC $C_{61}D_2$ Based on an Analytic Mean Field Approach

Wei Yang, Jiu-Xun Sun, and Li-Guo Wang

Department of Applied Physics, University of Electronic, Science and Technology, Chengdu 610054, P. R. China

Reprint requests to J.-X. S.; E-mail: sjx@uestc.edu.cn

Analytic expressions for the equation of state and internal energy of poly-exponential solids are derived based on the analytic mean field potential (AMFP) method. The formalism is applied to fcc $C_{61}D_2$. Two sets of potential parameters are determined by fitting the experimental compression data of $C_{61}D_2$ up to 1 GPa at 343 and 307 K, respectively. The difference between the two sets of parameters is small. Whereas the difference between the potential of the $C_{61}D_2$ molecules and that of the C_{60} molecules is fairly prominent, the conclusion is different from that in the literature, and the reason is unclear at present. The thermo-physical properties including the isothermals, thermal expansion, isochoric heat capacity, Helmholtz free energy and internal energy are calculated and analyzed. The theoretical results agree well with the experimental data available for solid $C_{61}D_2$.

Key words: AMFP; Morse Potential; Equation of State; Fullerene; Thermodynamic Properties.

1. Introduction

Over the past years, C_{60} and its derivatives have continued to attract considerable attention, due to both their elegant molecular structures and the intriguing structural, dynamic, and electronic properties of the solid phases of fullerenes. Pristine, C_{60}, has the form of a spherical shell, with 60 symmetrically equivalent carbon atoms [1]. At high temperature, the C_{60} molecules form a face-centered cubic (fcc) structure with free molecular rotation. Below 260 K the lattice transforms into a simple cubic (sc) structure with a temperature-(T) [2 – 4] and pressure- (P) [5, 6] dependent degree of molecular orientational order, which freezes into an orientational glass below 90 K [7]. The transitions, and structures of the high- and low-temperature phases have been the objects of numerous experimental and theoretical studies.

In order to study the thermodynamic properties of C_{60} better, several studies have recently been carried out on fullerenes modified by adding small side groups to decrease the symmetry of the molecule. The first step was to add only an oxygen atom to form the fullerene epoxide $C_{60}O$, the next to add instead the slightly larger CH_2 group to form $C_{61}H_2$ [7]. The effect of perturbing the icosahedral symmetry of C_{60} by the addition of the O or CH_2 side group upon orienta-

tional order-disorder and glass transitions in solid C_{60} has been studied by a combination of high-resolution capacitance dilatometry and single-crystal X-ray and powder inelastic neutron scattering. Both fullerene derivatives $C_{60}O$ (expoxide) and $C_{61}H_2$ (6.5-annulene) are shown to undergo a sequence of transitions similar to that found in pure C_{60}.

Although the structure and phase behaviour of $C_{61}H_2$ have been studied at zero-pressure [7, 8], little is known about its properties under high pressure, especially its thermodynamic properties at high temperature and pressure. Lundin et al. [7] have therefore investigated the equation of state of $C_{61}D_2$ (which should have physical properties practically identical to those of $C_{61}H_2$) using the same equipment [9] and method as applied previously to C_{60} [10, 11] and C_{70} [12]. Lundin et al. [7] have fitted the Murnaghan equation to their experimental data, and have found a linear dependence of the bulk modulus on the pressure within the whole experimental pressure range. Although the scatter in the data of the bulk modulus is prominent, they concluded that the addition of a CH_2 side group to C_{60} does not give a large effect on the bulk modulus, and the side group dwells in the intermolecular interactions remained those between C_{60} "bellies" [7]. The present paper is concerned with the calculation of the thermodynamic properties of fcc $C_{61}D_2$. The

research on the thermo-physical properties of solid $C_{61}D_2$ would be helpful for understanding the structure and phase properties of C_{60} and its derivatives. It is shown in the following sections that some conclusions deduced in the present paper are different from those of Lundin et al.

Several years ago, Wang et al. proposed the analytic mean field potential (AMFP) method [13–16], and they applied it to many materials. Bhatt et al. [17, 18] further applied the AMFP method to lead and alkali metals, and concluded that in comparison with other theoretical models the AMFP method is computationally simple, physically transparent and reliable in the study of thermodynamic properties at high pressures and high temperatures. Recently, Sun et al. proved that the AMFP method is an analytic approximation of the free volume theory (FVT) [19]. The FVT is a mean field approximation to the thermal contribution of atoms to the Helmholtz free energy of crystalline phases. Many authors have shown that the FVT can soundly include anharmonic terms which are important at high temperatures [20–22]. It is convenient to develop simple analytic equation of state (EOS) through the AMFP method in some cases, whereas the complete FVT fails. Sun have applied the AMFP method to solid C_{60} by the aid of the Girifalco potential [23]. The numerical results agree well with the MD simulations and are superior to the CUST of Zubov et al. [24, 25]. This verifies that the AMFP method is a convenient approach to consider the anharmonic effect at high temperatures.

As was pointed out by Girifalco [26, 27], the atoms in C_{60} molecules are held together by strong chemical bonds, while the interactions among these molecules in the fcc solid arise from van der Waals-type forces and are much weaker. To a good approximation, therefore, the thermal properties of fcc C_{60} can be treated as the sum of those resulting from intermolecular vibrations and those arising from intramolecular vibrations [26, 27]. Here we also mention the intermoleclear contributions for the solid fcc $C_{61}D_2$, as has been done by Girifalco [27] for C_{60}. Considering that the Girifalco potential [28–30] is too hard and gives compression curves prominently deviating from experiments at high pressure, whereas the Morse potential [31] can well describe the thermo-physical properties of most materials within wide pressure ranges, we utilize the double-exponential potential (an extended Morse potential) instead of the Girifalco potential.

The present paper is organized as follows. In Section 2 we derive an analytic equation of state based on the AMFP approach. In Section 3 the parameters of the double-exponential potential are determined by fitting experimental data of solid $C_{61}D_2$, and the numerical results are compared with experiments. In Section 4 the conclusion is presented.

2. Analytic Equation of State

In the poly-exponential potential

$$\varepsilon(s) = \varepsilon_0 \sum_{j=14}^{m} C_j \exp[\lambda_j(1 - r/r_0)] \tag{1}$$

r_0 is the equilibrium distance and ε_0 the well depth. For the double-exponential potential we have $m = 2$, and

$$C_1 = \lambda_2/(\lambda_1 - \lambda_2), \ C_2 = -\lambda_1/(\lambda_1 - \lambda_2). \tag{2}$$

The two parameters λ_1 and λ_2 describe the decay of the potential versus the radial coordinate r.

In terms of the FVT, the free energy can be expressed as [19, 23, 29, 30]

$$\frac{F}{NkT} = -\frac{3}{2}\ln(2\pi\mu kT/h^2) + \frac{u(0)}{2kT} - \ln v_\mathrm{f}, \tag{3}$$

where μ is the mass of the $C_{61}D_2$ molecule. $u(0)$ is the potential energy of a molecule, as the lattice is static, and v_f is the free volume:

$$u(0) = \sum_{i \neq 0} z_i \varepsilon\left(\frac{R_i}{r_0}\right) = \sum_{i \neq 0} z_i \varepsilon\left(\delta\frac{a}{r_0}\right)$$
$$= \sum_{i \neq 0} z_i \varepsilon(\delta_i y), \tag{4}$$

$$v_\mathrm{f} = 4\pi \int_0^{r_\mathrm{m}} \exp[-g(r,V)/kT]r^2\mathrm{d}r, \tag{5}$$

where $R_i = \delta_i a$ is the distance of molecules in the i-th shell with the centre molecule at $i = 0$, a is the nearest-neighbour distance. z_i and δ_i are structural constants (the values for the fcc structure have been given in [32]), $g(r,V)$ is the potential energy of a molecule as it roams from the centre to a distance r. In terms of the AMFP approach [13–19], $g(r,V)$ can be expressed by the static energy $E_\mathrm{c}(a)$ of a molecule:

$$g(r,V) = \frac{1}{2}\left[\left(1 + \frac{r}{a}\right)E_\mathrm{c}(a+r)\right.$$
$$\left. + \left(1 - \frac{r}{a}\right)E_\mathrm{c}(a-r) - 2E_\mathrm{c}(a)\right], \tag{6}$$

$$E_c(a) = \frac{1}{2}u(0) = \frac{1}{2}\sum_{i\neq 0} z_i \varepsilon(\delta, y). \tag{7}$$

$r_m = (3a^3/4\pi\gamma)^{1/3} \approx a/2$ is the Wigner-Seitz radius, which can be approximated by the largest displacement of the centre molecule. γ is the structure constant; for the fcc structure it is $\sqrt{2}$.

The volume of a fcc solid is $V = Na^3/\gamma$. For simplicity, we introduce the dimensionless reduced free volume $\tilde{v}_f$, the reduced volume y, and the reduced radial coordinate x as follows:

$$v_f = 4\pi a^3 \tilde{v}_f = 4\pi\gamma V \tilde{v}_f, \tag{8}$$

$$y = a/r_0 = (V/V_0)^{1/3}, \tag{9}$$

$$V_0 = N(r_0)^3/\gamma, \tag{10}$$

$$x = r/a, \quad x_m = \frac{r_m}{a} \approx \frac{1}{2}. \tag{11}$$

The reduced free volume $\tilde{v}_f$ and its derivatives with respect to temperature and reduced volume can be expressed as

$$\tilde{v}_f = \int_0^{x_m} \exp[-g(x,y)/kT]x^2 dx, \tag{12}$$

$$\begin{aligned}\tilde{v}_{fa} &= T\frac{\partial}{\partial T}\tilde{v}_f \\ &= \frac{1}{kT}\int_0^{x_m} \exp[-g(x,y)/kT]g(x,y)x^2 dx,\end{aligned} \tag{13}$$

$$\begin{aligned}\tilde{v}_{fb} &= -\frac{\partial}{\partial y}\tilde{v}_f \\ &= \frac{1}{kT}\int_0^{x_m} \exp[-g(x,y)/kT]\frac{\partial}{\partial y}g(x,y)x^2 dx.\end{aligned} \tag{14}$$

Here $g(x,y) \equiv g(r,V)$. Combining (5), (8) and (11), we have

$$\begin{aligned}g(x,y) &\equiv g(r,V) \\ &\approx \frac{1}{4}\sum_{i\neq 0} z_i \Big[(1+x)\varepsilon(\delta_i y + \delta_i yx) \\ &\quad + (1-x)\varepsilon(\delta_i y - \delta_i yx) - 2\varepsilon(\delta_i y)\Big],\end{aligned} \tag{15}$$

$$\begin{aligned}\frac{\partial}{\partial y}g(x,y) &\approx \frac{1}{4}\sum_{i\neq 0} z_i\delta_i\Big[(1+x)^2\varepsilon'(\delta_i y + \delta_i yx) \\ &\quad + (1-x)^2\varepsilon'(\delta_i y - \delta_i yx) - 2\varepsilon'(\delta_i y)\Big],\end{aligned} \tag{16}$$

$$\varepsilon'(s) = -\varepsilon_0 \cdot \sum_{j=1}^{m} \lambda_j C_j e^{\lambda_j(1-s)}. \tag{17}$$

The compressibility factor and internal energy can be derived as

$$Z = \frac{PV}{NkT} = -\frac{y}{3}\frac{\partial}{\partial y}\frac{f}{NkT} = \frac{P_c V}{NkT} + \frac{P_f V}{NkT}, \tag{18}$$

$$\frac{P_c V}{NkT} = -\frac{y}{6kT}\frac{\partial}{\partial y}u(0), \tag{19}$$

$$\frac{\partial}{\partial y}u(0) = \sum_{i\neq 0} z_i\delta_i\varepsilon'(\delta_i y), \tag{20}$$

$$\frac{P_f V}{NkT} = 1 + \frac{y}{3\tilde{v}_f}\frac{\partial}{\partial y}\tilde{v}_f = 1 - \frac{y\tilde{v}_{fb}}{3\tilde{v}_f}, \tag{21}$$

$$\begin{aligned}\frac{U}{NkT} &= -T\frac{\partial}{\partial T}\frac{F}{NkT} = \frac{3}{2} + \frac{u(0)}{2kT} + \frac{T}{\tilde{v}_f}\frac{\partial \tilde{v}_f}{\partial T} \\ &= \frac{3}{2} + \frac{u(0)}{2kT} + \frac{\tilde{v}_{fa}}{\tilde{v}_f},\end{aligned} \tag{22}$$

where P_c is the cold pressure and P_f the thermal pressure deduced from the free volume.

By using the above equations, all other thermodynamic quantities can be analytically derived. The derivations are straightforward. However, the expressions for the thermal expansion coefficient, compressibility coefficient and isochoric heat capacity are redundant; we would calculate these quantities by using numerical differentiation instead of the analytic expressions. The compressibility factor can be seen as a function of the variables y and T, $Z = Z(y,T)$. In terms of the function, the formulas for the thermal expansion coefficient, compressibility coefficient and isochoric heat capacity can be reduced to the following form:

$$\begin{aligned}\alpha &= \frac{1}{V}\left(\frac{\partial V}{\partial T}\right)_P = \frac{3}{y}\left(\frac{\partial y}{\partial T}\right)_P \\ &= \left[\frac{Z}{T} + \left(\frac{\partial Z}{\partial T}\right)_y\right]\left[Z - \left(\frac{y}{3}\right)\left(\frac{\partial Z}{\partial y}\right)_T\right]^{-1},\end{aligned} \tag{23}$$

$$\begin{aligned}\beta &= -\frac{1}{V}\left(\frac{\partial V}{\partial P}\right)_T = -\frac{3}{y}\left(\frac{\partial y}{\partial P}\right)_T \\ &= \left(\frac{V_d y^3}{NkT}\right)\left[z - \left(\frac{y}{3}\right)\left(\frac{\partial Z}{\partial y}\right)_T\right]^{-1},\end{aligned} \tag{24}$$

$$\frac{C_V}{Nk} = \frac{1}{Nk}\left(\frac{\partial U}{\partial T}\right)_V = \frac{u}{NkT} + T\frac{\partial}{\partial T}\left(\frac{U}{NkT}\right)_y. \tag{25}$$

In our calculations it is found that following the steps of the numerical differentiations in (23)–(25) can reach stable numerical results, $\Delta T = 0.00001 \cdot T$ and $\Delta y = 0.00001 y$.

3. Numerical Results and Discussion

In this section we apply the above formalism to fcc $C_{61}D_2$. We notice that one nonphysical phenomenon exists in the original experimental data of Lundin et al. [7]. In terms of the thermodynamic laws, the pressure should be an increasing function of the temperature. However, the experimental data of Lundin et al. [7] showed the contrary tendency, i. e. the pressure decreases as the temperature increases, as shown in Figure 1. They [7] have not explained the abnormal phenomena. Lundin et al. [7] gave three sets of experimental data at 175, 307 and 343 K. Their analysis exhibited that the solid $C_{61}D_2$ can exist in an sc and fcc phase at low- and high-temperature regions, and the sc-to-fcc transformation temperature is about 290 K. In terms of these results, we propose a possible explanation for the abnormal phenomena. At 175 K solid $C_{61}D_2$ exists in the sc phase; it has a low density. At 343 K solid $C_{61}D_2$ exists in the fcc phase; it has a high density. As the two phases have compressed to the same high density, the sc phase must have a higher compression ratio V/V_0 than the fcc phase; thus the sc phase (at low temperature) has a higher pressure than the fcc phase (at high temperature). At 307 K solid $C_{61}D_2$ may exist as a mixture of sc and fcc phases. The corresponding compression curve locates between the two curves at 175 and 343 K. Because our work mainly aimed to fit the experimental data by using the AMFP method approach and predict other thermodynamic properties of $C_{61}D_2$, we feel it is difficult to give a sound explanation for the abnormal phenomena within the AMFP method theoretical framework of this paper. However, we think the present work may provide some issues for solving the problem.

Considering the three isothermals measured by Lundin et al. [7] at three temperatures (175, 307 and 343 K) and that the sc-to-fcc phase transition temperature of $C_{61}H_2$ is about 290 K, we do not use the experimental data at 175 K, since at this temperature $C_{61}D_2$ may freeze into an orientational glass. Although we have tried to fit the data at 307 and 343 K at same time, the fitting precision was not satisfactory. We thus determined two sets of parameters for the double-exponential potential by fitting the data at 307
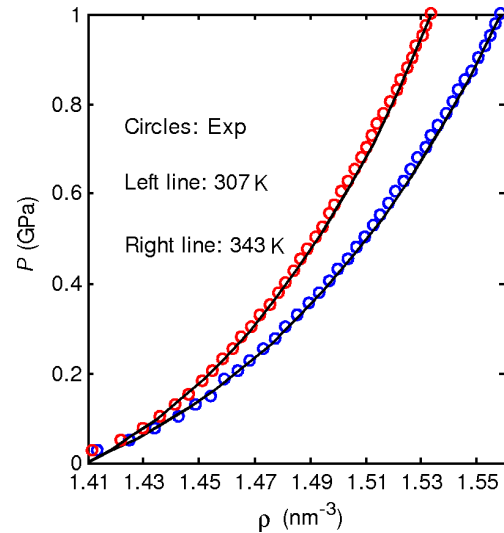

Fig. 1. Pressure as a function of density for fcc $C_{61}D_2$ at 343 K and 307 K by using the parameters of (26) and (27), respectively. Comparison of the results of our calculation (lines) with the experimental data (circles).

and 343 K, respectively. The experimental data and smoothed fitting curves are plotted in Figure 1. The figure shows that the fitting precision is satisfactory. The determined values of the parameters are as follows:

$$\lambda_1 = 2.84, \quad \lambda_2 = 46.2,$$
$$r_0 = 1.0092 \text{ nm}, \quad \varepsilon_0 = 1660 \text{ K (343 K)}, \tag{26}$$

$$\lambda_1 = 2.70, \quad \lambda_2 = 54.0,$$
$$r_0 = 1.0094 \text{ nm}, \quad \varepsilon_0 = 1710 \text{ K (307 K)}. \tag{27}$$

Equations (26) and (27) show that the difference between the two sets of parameters is small except for λ_2 the difference of which is about 20%.

Lundin et al. [7] have used the Murnaghan EOS to analyze their experimental data, and found that the bulk modulus at zero-pressure and 307 K is 6.4 GPa, which was in agreement with the value 6.8 GPa of solid C_{60} measured by themselves. Combining the lattice constant 1.419 nm of $C_{61}H_2$ at ambient temperature is in accordance with that of solid C_{60}, they concluded that the side groups dwell in intermolecular voids in the lattice and the main intermolecular interactions remain those between C_{60} "bellies". However, in Fig. 2 we plot the potentials for $C_{61}D_2$ molecules and C_{60} molecules. The figure shows that the well depth of C_{60} molecules is about 3200 K, deduced from both the Girifalco potential and the double-Yukawa potential [26, 30], far larger than 1660 and 1710 K given

Table 1. Thermo-physical properties of the fcc phase of $C_{61}D_2$ at zero-pressure calculated by using the parameters determined from the experimental data at 343 K: the lattice constant a in nm, the linear thermal expansion coefficient α in 10^{-5} K^{-1}, the bulk modulus B_T in kbar, the heat capacity C_V in $kJ \cdot mol^{-1} \cdot K^{-1}$.

T	a	α	B_T	C_V
100	1.4054	2.7581	54.081	24.187
200	1.4094	2.9840	46.882	23.497
400	1.4186	3.5519	34.505	22.191
600	1.4298	4.3234	24.563	20.947
800	1.4436	5.3795	16.824	19.742
1000	1.4612	6.8409	11.031	18.577
1200	1.4843	8.9485	6.8410	17.465
1400	1.5158	12.440	3.8450	16.416
1600	1.5647	20.964	1.6585	15.399
1700	1.6074	36.382	0.7549	14.846
1760	1.6638	118.90	0.1763	14.387
1768	1.6922	808.96	0.0229	14.235

Table 2. The same as for Table 1, but the parameters are determined from the experimental data at 307 K.

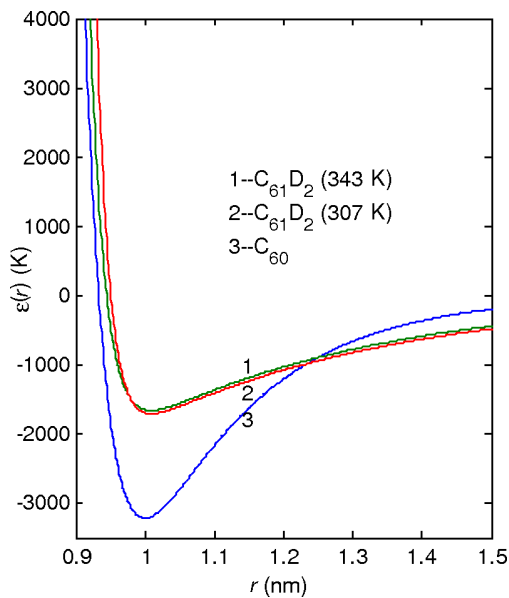| T	a	α	B_T	C_V
100	1.4073	2.6030	65.856	24.112
200	1.4111	2.8283	56.511	23.361
400	1.4199	3.3923	40.789	21.955
600	1.4305	4.1429	28.588	20.637
800	1.4438	5.1246	19.467	19.392
1000	1.4604	6.3887	12.910	18.232
1200	1.4816	8.0564	8.2952	17.175
1400	1.5090	10.534	5.0167	16.230
1600	1.5475	15.314	2.6178	15.371
1800	1.6163	34.196	0.7872	14.515
1850	1.6529	63.106	0.3564	14.251
1877	1.7180	744.98	0.0234	14.010

Fig. 2. Comparison of the double-Yukawa potential of the C_{60} molecules [30] with that of the $C_{61}D_2$ molecules by using the parameters of (26) and (27), respectively.
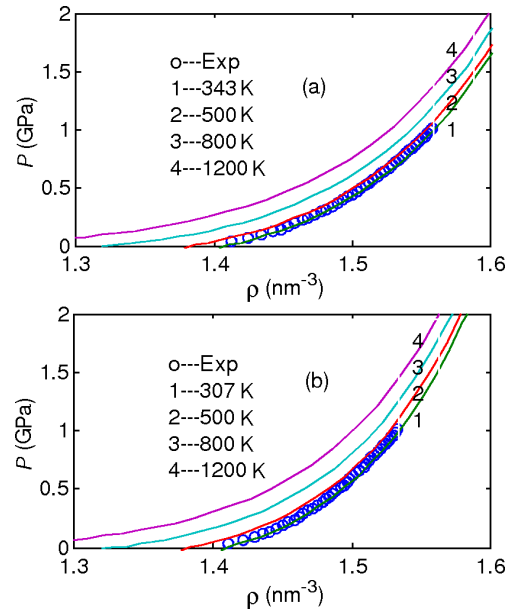

Fig. 3. Isothermal curves at 343 K (a) [or 307 K (b)], 500 K, 800 K, 1200 K calculated by using the parameters of (26) and (27), respectively. The circles (○) are experimental data.

by (26) and (27) of $C_{61}D_2$ molecules. The result is different from the conclusion of Lundin et al. [7], and shows that the intermolecular interaction between the $C_{61}D_2$ molecules deduced from the experimental data available at present is weaker than that between the C_{60} molecules.

In Tables 1 and 2, the calculated thermodynamic properties at zero-pressure and different temperatures by using the parameters (26) and (27) are listed, respectively. The spinodal point T_s is the temperature sat-

isfying the condition $B_T(T_s) = 0$. The system is instable for temperatures above T_s. From the two tables we know that T_s is 1768 K and 1877 K for the parameters (26) and (27), respectively. The two tables show that the thermal expansion coefficient is an increasing function of the temperature, whereas the bulk modulus and the isochoric heat capacity are decreasing functions of the temperature. The thermal expansion coefficient becomes divergent and the bulk modulus tends to zero near the spinodal temperatures.

In Figs. 3–8, the results of thermodynamic properties of solid fcc $C_{61}D_2$ calculated by using the double-exponential potential are plotted. The isother-
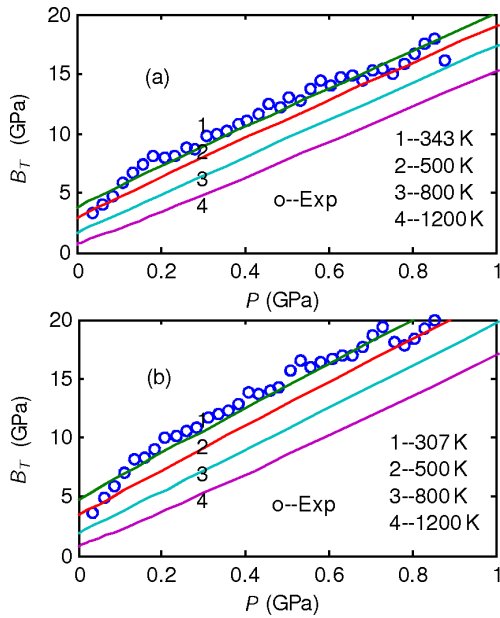
Fig. 4. Variations of the bulk modulus B_T versus the pressure P at the same temperatures as in Figure 3. The circles ($\circ$) are experimental data.
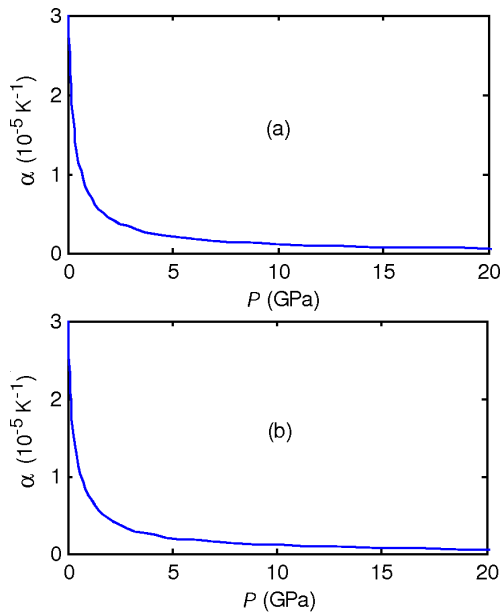

Fig. 5. Variation of the thermal expansion coefficient α versus the pressure P calculated by using the parameters of (26) and (27), respectively.

Fig. 6. Variation of the isochoric heat capacity C_V versus the pressure P calculated in this work.

Fig. 7. Variation of the free energy F versus the density ρ at 343 K (a) [or 307 K (b)], 500 K, 800 K, 1200 K calculated by using the parameters of (26) and (27), respectively.

mal curves at 343 K (or 307 K), 500 K, 800 K, 1200 K calculated by using the parameters (26) and (27), respectively, are plotted in Figure 3. The variations of
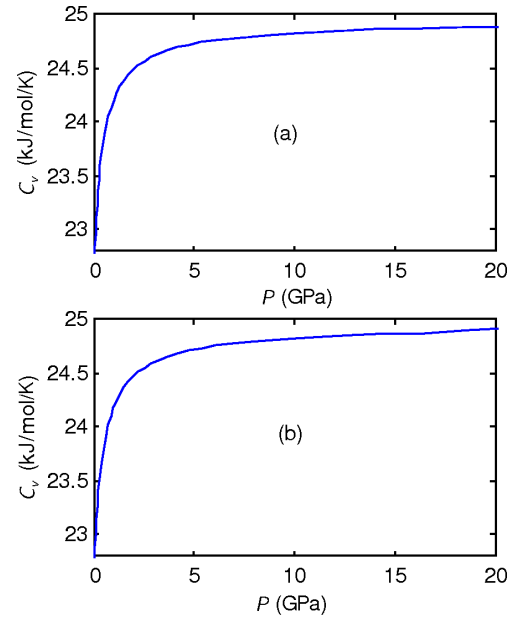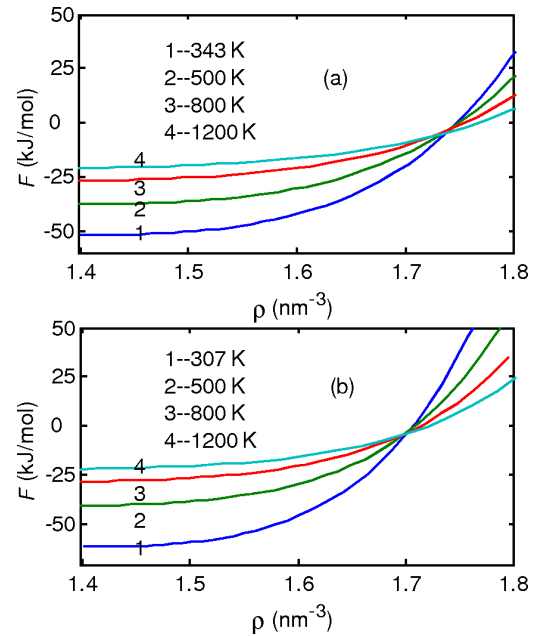
the bulk modulus versus pressure at the same temperatures are plotted in Figure 4. In the two figures, the experimental data available are also plotted for compar-
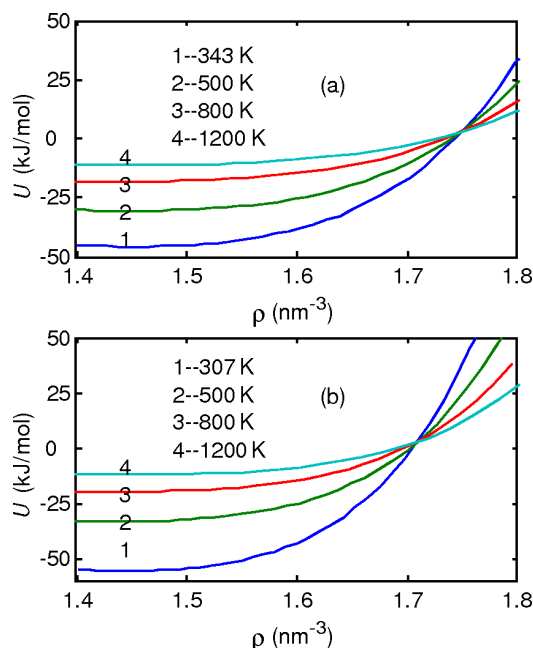
Fig. 8. The same as for Fig. 7, but for the internal energy U.

ison as well as the isothermal curves at 500 K, 800 K and 1200 K. The two figures show that the agreement of theoretical results with experiments is satisfactory. The difference between the variations of pressure versus density and bulk modulus versus pressure, calculated from the two sets of parameters, is small at low density or pressure, and slightly enlightened at high density or pressure conditions. But overall speaking, the difference is not prominent.

Figures 5 and 6 plot the variation of the thermal expansion coefficient α and isochoric heat capacity C_v versus pressure P at 343 K and 307 K, respectively. Figure 5 shows that α is a decreasing function of pressure; at low pressure the variation is fast, but at high

pressure, the variation slows down and shows some saturation effect. Figure 6 shows that C_v is an increasing function of pressure, and the variation is fast at low pressure and slow at high pressure. Figures 7 and 8 plot the variation of the free energy F and internal energy U versus density ρ at four temperatures. The two figures show that F and U are increasing functions of density for all temperatures, and the variation at low temperatures is faster than that at high temperatures. However, F and U are increasing functions of temperature at low-density condition. And the situation changes as the density increases; F and U become decreasing functions of temperature at high density.

4. Conclusion

In summary, expressions on the equation of state and internal energy for a poly-exponential solid have been derived, based on the AMFP method. The formalism was applied to solid fcc $C_{61}D_2$. Two sets of potential parameters were determined through fitting the experimental compression data of $C_{61}D_2$ up to 1 GPa and at 343 and 307 K, respectively. The difference between the two sets of parameters was small, whereas the difference between the potential for the $C_{61}D_2$ molecules and that for the C_{60} molecules was fairly prominent. The reason is unclear at present. The calculated results agree well with the experimental data available for solid $C_{61}D_2$. We think it is very necessary to make more investigations on solid $C_{61}D_2$.

[1] M. R. Stetzer, P. A. Heiney, P. W. Stephens, R. E. Dinnebier, Q. Zhu, R. M. Strongin, B. M. Brandt, and A. B. Smith III, Phys. Rev. B **62**, 9305 (2000).
[2] J. D. Axe, S. C. Moss, and D. A. Neumann, in: Solid State Physics (Eds. H. Ehrenreich and F. Spaepen), Academic Press, New York 1994, Vol. 48, p. 150.
[3] P. A. Heiney and J. E. Fischer, J. Phys. Chem. Solids **54**, 1725 (1993).
[4] P. A. Heiney, J. E. Fischer, A. R. McGhie, W. J. Romanow, A. M. Denenstein, J. P. McCauley, Jr., and A. B. Smith, Phys. Rev. Lett. **66**, 2911 (1991).

[5] W. I. F. David and R. M. Ibberson, J. Phys. Condens. Matter **5**, 7923 (1993).
[6] B. Sundqvist, Solid State Commun. **93**, 109 (1995).
[7] A. Lundin, A. Soldatov, B. Sundqvist, R. M. Strongin, L. Brard, J. E. Fischer, and A. B. Smith III, Carbon **34**, 1119 (1996).
[8] C. Meingast, G. Roth, L. Pintschovius, R. H. Michel, C. Stoermer, M. Kappes, P. A. Heiney, L. Brard, R. M. Strongin, and A. B. Smith III, Phys. Rev. B **54**, 124 (1996).

[9] A. Lundin, R. G. Ross, and G. Backstrom, High Temp. High Pressures **26**, 477 (1994).

[10] A. Lundin and B. Sundqvist, Europhys. Lett. **27**, 463 (1994).

[11] A. Lundin and B. Sundqvist, Phys. Rev. B **53**, 8329 (1996).

[12] A. Lundin, A. Soldatov, and B. Sundqvist, Europhys. Lett. **30**, 469 (1995).

[13] Y. Wang, D. Chen, and X. Zhang, Phys. Rev. Lett. **84**, 3220 (2000).

[14] Y. Wang, Phys. Rev. B **62**, 196 (2000).

[15] Y. Wang, Phys. Rev. B **63**, 245108 (2001).

[16] Y. Wang, R. Ahuja, and B. Johansson, Phys. Rev. B **65**, 014104 (2001).

[17] N. K. Bhatt, A. R. Jani, P. R. Vyas, and V. B. Gohel, Physica B **65**, 014104 (2001).

[18] N. K. Bhatt, P. R. Vyas, A. R. Jani, and V. B. Gohel, J. Phys. Chem. Solids **66**, 797 (2005).

[19] J. X. Sun, L. C. Cai, Q. Wu, and F. Q. Jing, Phys. Rev. B **71**, 024107 (2005).

[20] E. R. Cowley, J. Gross, Z. Gong, and G. K. Horton, Phys. Rev. B **42**, 3135 (1990).

[21] E. Wasserman and L. Stixrude, Phys. Rev. B **53**, 8296 (1996).

[22] J. X. Sun, H. C. Yang, Q. Wu, and L. C. Cai, J. Phys. Chem. Solids **63**, 113 (2002).

[23] J. X. Sun, Physica B **12**, 268 (2005).

[24] V. I. Zubov, N. P. Tretiakov, J. F. Sanchez, and A. A. Caparica, Phys. Rev. B **53**, 12080 (1996).

[25] V. I. Zubov, J. F. Sanchez-Ortiz, N. P. Tretiakov, and I. V. Zubov, Phys. Rev. B **55**, 6747 (1997).

[26] L. A. Girifalco, J. Phys. Chem. **96**, 858 (1992).

[27] L. A. Girifalco, Phys. Rev. B **52**, 9910 (1995).

[28] M. C. Abramo, C. Caccamo, D. Costa, G. Pellicane, and R. Ruberto, Phys. Rev. E **69**, 031112 (2004).

[29] J. X. Sun, L. C. Cai, Q. Wu, and F. Q. Jing, Phys. Rev. B **73**, 155431 (2006).

[30] J. X. Sun, Phys. Rev. B **75**, 035424 (2007).

[31] A. I. Karasevskii and W. B. Holzapfel, Phys. Rev. B **67**, 224301 (2003).

[32] N. X. Chen, Z. D. Chen, and Y. C. Wei, Phys. Rev. E **55**, R5 (1997).